2006-01-01

A Case Study in Modeling and Process Control: the Control of a Pilot Scale Heating and Ventilation System

Robin Mooney
Technological University Dublin, robin.mooney@mydit.ie

Aidan O'Dwyer
Technological University Dublin, aidan.odwyer@tudublin.ie

A CASE STUDY IN MODELLING AND PROCESS CONTROL: THE CONTROL OF A PILOT SCALE HEATING AND VENTILATION SYSTEM

Robin Mooney and Aidan O'Dwyer *

School of Control Systems and Electrical Engineering, Dublin Institute of Technology, Kevin St., Dublin 8, Ireland (* Principal author. E-mail: aidan.odwyer@dit.ie).

ABSTRACT

This paper details the control of a pilot scale laboratory heating and ventilation system. The system is represented in 2x2 multi-input, multi-output (MIMO) form. A process reaction curve identification technique was used to model (in first order lag plus delay - FOLPD - form) the flow process and temperature process portions of the system, over a range of operating conditions. Tests revealed that both processes were continuously non-linear. A gain scheduler with static decoupling was designed, using look-up tables, to continuously interpolate for the most suitable proportional-integral (PI) or proportional-integral-derivative (PID) controller settings and decoupler gains. The contribution of this paper is the careful application, using well-known techniques, of a complete controller design cycle for a laboratory scale system.

KEYWORDS: MIMO, non-linear process, gain scheduling.

1. INTRODUCTION

The VVS-400 process, from Instrutek A/S, Larvik, Norway [1], is a pilot scale heating and ventilation system. A schematic diagram of the system is shown in Figure 1, with a three dimensional diagram of the system shown in Figure 2.

Figure 1: Schematic diagram of the Instrutek VVS-400 heating and ventilation rig

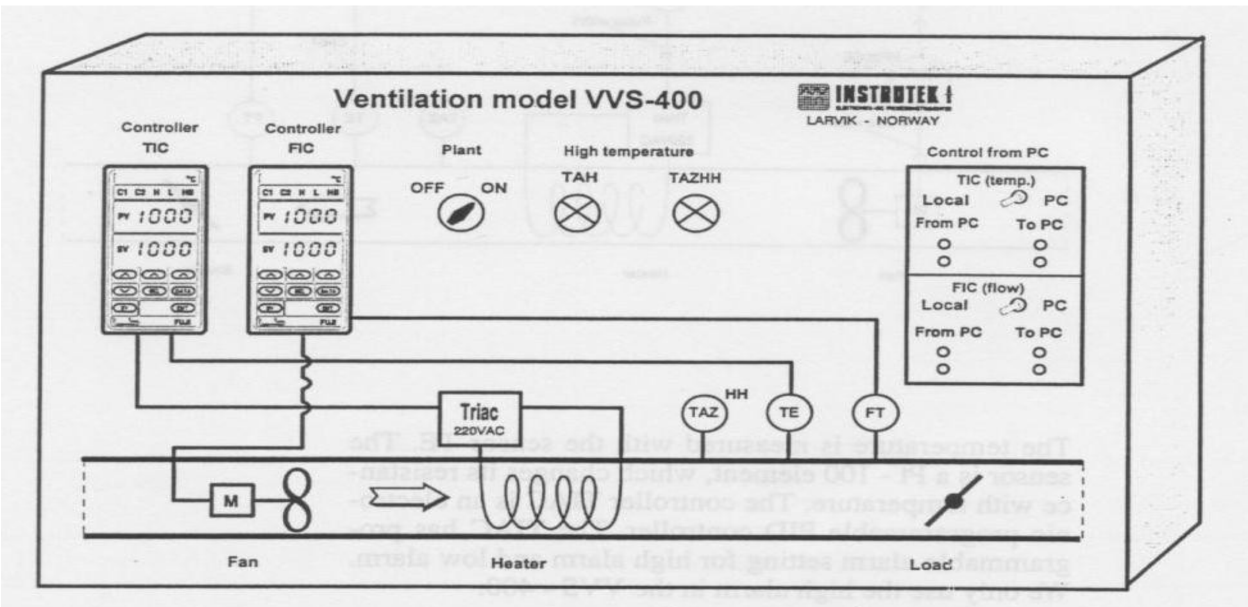

Figure 2: Three-dimensional diagram of the Instrutek VVS-400 heating and ventilation rig

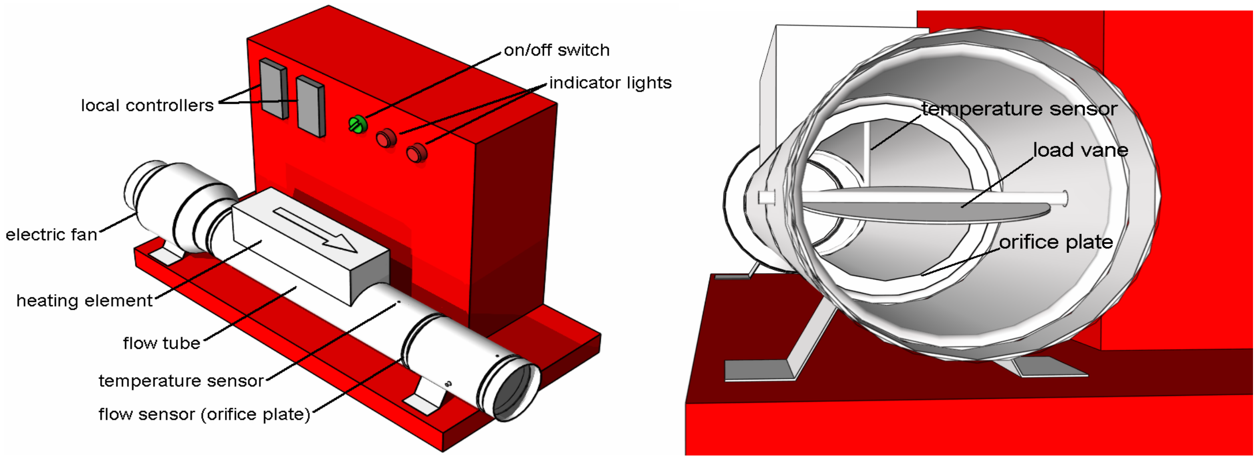

(a) Overview (b) End-elevation view

An electric fan is located at one end of a non-insulated metal tube (painted white). The fan blows air over a heating element. The air exits to the surroundings at the other end of the tube. An orifice plate is situated just before the exit (see end-elevation view, Figure 2). The differential pressure across the orifice is used to determine the flow rate. A platinum resistance temperature sensor is positioned inside the tube. A load vane provides a method of restricting the airflow at the tube exit. The power supply and other electrical components of the rig are inside the housing. Two independent local controllers (Fuji PY25) for the flow and temperature processes, that have PID and auto-tuning functions, are provided. It is possible to connect directly to the fan and the heating element, switching out the local controllers, so that the processes may be P.C. controlled.

The process has been used as a platform to test an identification strategy [2] or to compare generalised predictive control (GPC) and PID control design approaches [3], [4]. However, to the author's knowledge, no complete controller design cycle, from process modelling to appropriate controller implementation, has been reported on the process. Work on such a controller design cycle is reported in this paper. Firstly, a simple, non-model based approach is attempted (Section 2). Due to the inadequate results obtained, the results of a more detailed study, comprising process model identification (Section 3), process nonlinearity investigation (Section 4) and subsequent controller design (Section 5), are reported. Finally, conclusions and recommendations are drawn.

2. NON-MODEL BASED CONTROL

PI or PID controllers, for both the temperature and flow processes, may be implemented using the appropriate local controllers, either in autotune mode or using, for example, an ultimate cycle experimental approach [5]. Alternatively, the rig comes with a dedicated data acquisition card and software to allow P.C. based controller tuning. However, the control achieved, with either the local or P.C. based controller, was disappointing. Firstly, the slow response of the temperature process meant that an experimental approach was practically difficult. For the faster flow process, it is possible to quickly obtain PI controller settings, for example; indicative results are shown in Figures 3 to 5. In this ultimate cycle test, the flow controller set-point was put to 30% of its maximum value, with the load vane fully open. Following the ultimate cycle procedure [5], integral and derivative settings were put to zero, and the proportional band of the controller was gradually decreased until sustained oscillations occurred in the measured flow (Figure 3). Controller parameters (proportional band of 99% and integral time of 18 seconds) were subsequently determined. Servo responses with these controller settings were recorded (Figures 4 and 5).

Figure 3: Sustained oscillations in measured flow recorded

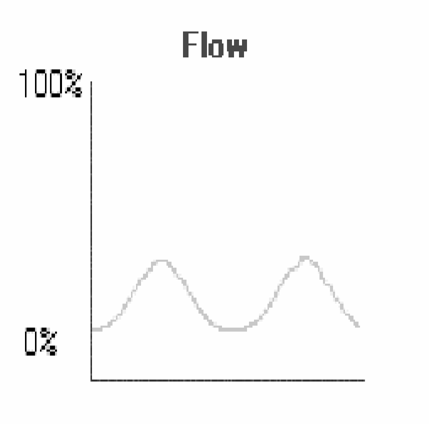

Figure 4: Servo response: 30%-50% command

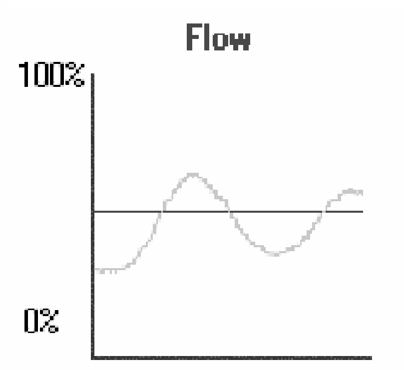

Figure 5: Servo response: 50%-30% command

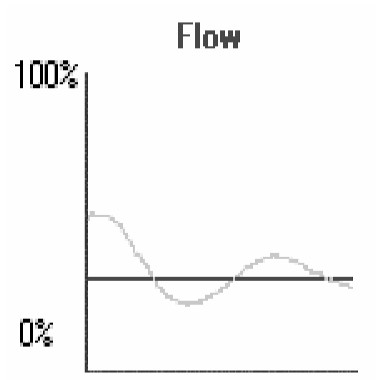

The results in Figures 4 and 5 are poor, though they were better than those obtained in autotune mode. These results could be improved by subsequent manual tuning. However, there is also evidence of non-linear behaviour, backed up by subsequent experimental work. The full panorama of results obtained suggested that adequate controller parameters would depend on process operating conditions. These results provided the motivation for a more detailed study.

3. PROCESS MODEL IDENTIFICATION

Process models were determined, from the open loop step response of both the flow process and the temperature process, using the alternative tangent and point method of Ziegler and Nichols [6], over a range of operating conditions. After some preliminary tests, three flow process models were specified corresponding to "low", "medium", and "high" flow settings ("low" is specified as fan voltage setting < 55% of maximum, "medium" is specified as fan voltage setting in the range 55% to 75% of maximum, with "high" being specified as fan voltage setting > 75% of maximum). Table 1 shows a summary of all the flow process models obtained.

Table 1: All flow process models obtained

Model	$G_{m_{LOW-FLOW}}(s) = \dfrac{0.45e^{-0.98s}}{1+2.70s}$	$G_{m_{MED-FLOW}}(s) = \dfrac{1.08e^{-1.08s}}{1+1.93s}$	$G_{m_{HIGH-FLOW}}(s) = \dfrac{1.76e^{-0.93s}}{1+1.45s}$

The temperature process characteristics depend on the flow process. Nine models of the temperature process were determined corresponding to "low", "medium", and "high" heater settings, at three different flow rates (for the temperature process, "low" is specified as heater setting < 45% of maximum, "medium" is specified as heater setting in the range 45% to 65% of maximum, with "high" specified as heater setting > 65% of maximum). All the temperature process models obtained are shown in Table 2.

Table 2: All temperature process models obtained

Models (30% Flow)	$G_{m_{LOW-TEMP}}(s) = \frac{0.32e^{-32s}}{1+124s}$	$G_{m_{MED-TEMP}}(s) = \frac{0.61e^{-22s}}{1+153s}$	$G_{m_{HIGH-TEMP}}(s) = \frac{0.45e^{-24s}}{1+150s}$
Models (50% Flow)	$G_{m_{LOW-TEMP}}(s) = \frac{0.32e^{-16s}}{1+123s}$	$G_{m_{MED-TEMP}}(s) = \frac{0.43e^{-16s}}{1+109s}$	$G_{m_{HIGH-TEMP}}(s) = \frac{0.30e^{-17s}}{1+113s}$
Models (70% Flow)	$G_{m_{LOW-TEMP}}(s) = \frac{0.30e^{-22s}}{1+99s}$	$G_{m_{MED-TEMP}}(s) = \frac{0.41e^{-23s}}{1+101s}$	$G_{m_{HIGH-TEMP}}(s) = \frac{0.33e^{-19s}}{1+119s}$

It is obvious from the process identification performed that both the flow and temperature processes are non-linear. A static characteristic curve for each process was obtained to investigate this further. The process was interfaced with a computer via a data acquisition board, which accepts 0-5V; inputs and outputs recorded are subsequently normalised. The resulting flow process curve (Figure 6) shows that limits exist on its maximum and minimum operating region. At flows less than 15% of maximum fan voltage setting (labelled as input flow in Figure 6), very little change in measured flow (labelled as output flow in Figure 6) occurs for a change in input. This is effectively a dead-band region of the flow. The figure also shows that the slope of the characteristic curve is greater at high inputs, implying high process model gain at high inputs (this is compatible with the results reported in Table 1). The temperature process has an infinite number of characteristic curves, as process behaviour depends on the infinite number of possible flow rates. Characteristic curves at three flow rates were determined (Figure 7).

Figure 6: Flow process characteristic curve

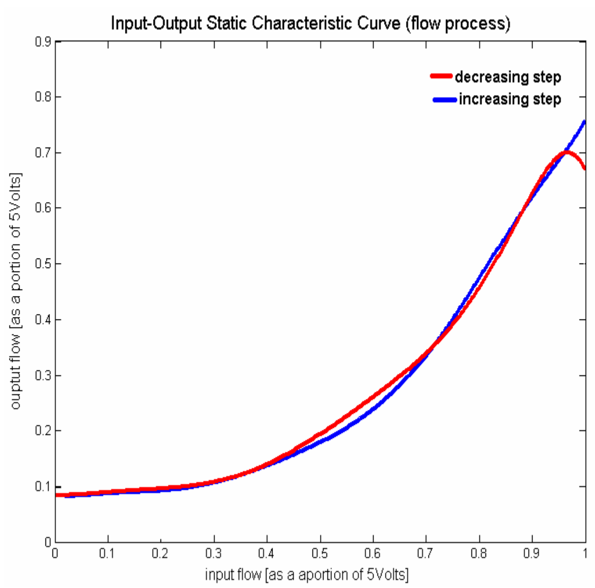

Figure 7: Temperature process characteristic curve

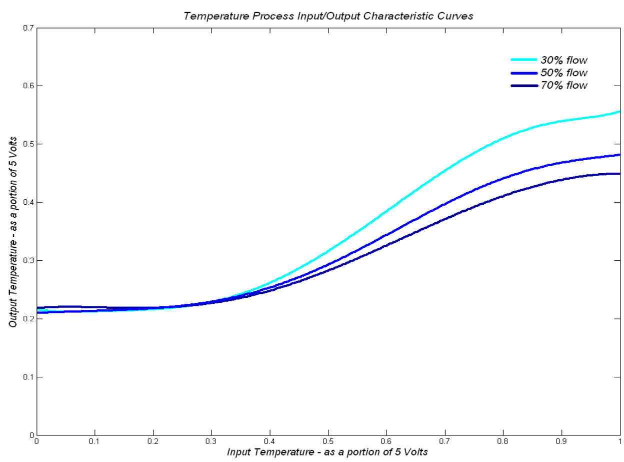

It is clear that the higher the flow rate, the lower the maximum temperature achievable. This is sensible from an intuitive point of view as the cooling effect of the airflow would be greater at high flow rates. At high heater settings (labelled as input temperature in Figure 7), each curve tended to level off or saturate; the maximum temperature obtainable is limited by the maximum power output of the element. Each curve has a lower limit consistent with the ambient room temperature.

4. INVESTIGATION INTO PROCESS INTERACTIONS

If the dynamics of one process affect the dynamics of the other, then a process interaction exists. Process interactions can lead to difficulties when designing effective controllers for each process. To examine the possibility of process interactions in the application, two simple tests were carried out. In each case, the input to both processes was held constant and allowed to settle. Then one of the process inputs underwent a step change; the output of the other process was observed. Figure 8 shows the results from both tests. The left hand plot shows the result when the temperature process input (i.e. heater setting) is held constant (at 0.5) and the flow process input (i.e. fan voltage) undergoes a step change; the output (measured) temperature reduces considerably (from $0.45 \equiv 45°C$ to $0.31 \equiv 31°C$). It should be noted that the change in flow was considerable (from 15% to 75% of full range), representing close to a worst-case scenario. The right hand plot shows that when the flow process input is held constant and the temperature process input undergoes a step change, the (measured) flow process output remains undisturbed.

Figure 8: Interaction between the processes

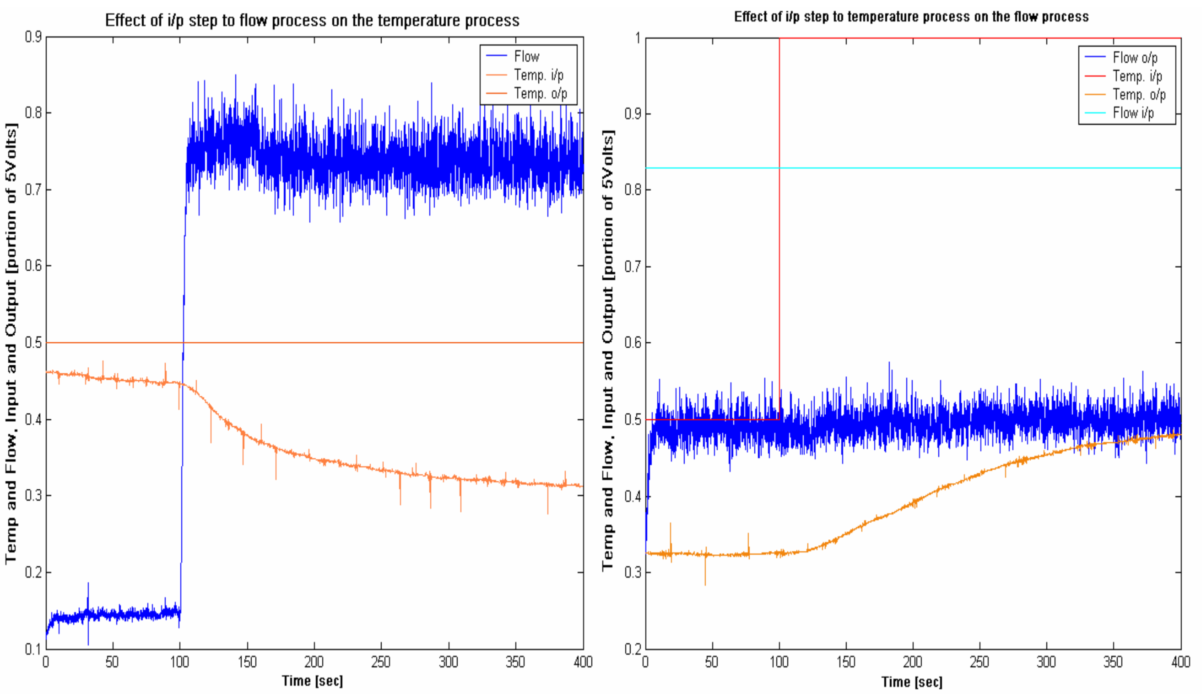

The results show that the temperature process dynamics depend on the operating conditions of the flow process, but the flow process dynamics are unaffected by the operating conditions of the temperature process (as expected). The models obtained for the interaction transfer function, labelled G_{FT} (at three heater settings) are shown in Table 3.

Table 3: Interaction models obtained

Interaction Models	$G_{FT-LowTemp}(s) = \frac{-0.02e^{-16s}}{1+63s}$	$G_{FT-Med.Temp}(s) = \frac{-0.18e^{-8s}}{1+85s}$	$G_{FT-HighTemp}(s) = \frac{-0.24e^{-7s}}{1+70s}$

As expected, it was found that the model gain was negative, i.e. increasing flow leads to decreased temperature. The effect of the interaction was greater at high temperatures. A static decoupler was designed, using a standard method (as described, for example, by Seborg *et al.* [7]), to reduce the effect of the interaction.

5. CONTROLLER DESIGN

PI or PID controllers were chosen to control the processes because of the relatively low time delay to time constant ratio revealed by the identification tests, their wide use in industry and relatively simple implementation. Suitable tuning rules were chosen for these controllers, based on minimising the integral of absolute error (IAE) performance criterion, for both servo and regulator applications [8]. The controllers were specified for each operating point; full results are provided by Mooney [9]. Preliminary closed loop response tests were carried out at particular operating conditions. Servo and regulator performance for the "medium" flow condition, and separately for the "medium" temperature condition, at 30% flow condition, are provided in Figures 9 and 10, respectively. Satisfactory performance is observed.

A gain scheduler was then designed to switch between controller settings. The implementation platform is based on HUMUSOFT/MATLAB/SIMULINK, with appropriate data acquisition. Due to space restrictions, only the results associated with the gain scheduled PI controller will be presented. Full details of the results associated with the gain scheduled PID controller, and the design of the gain schedulers, will be presented at the conference.

Tests were carried out comparing the gain scheduler to a fixed parameter PI controller implementation with controller settings based on an average model of the flow and temperature process. Sample results are shown in Figure 11 (flow controller, PI regulator) and Figure 12 (temperature controller, PI servo). In these results, "Advanced Gain Scheduler" refers to the gain scheduler implementation, and "Average Model Controller" refers to the fixed parameter PI controller implementation.

Over the full panorama of implementation results [9], the gain scheduler produced better performance, as expected.

Figure 9: Responses – flow system

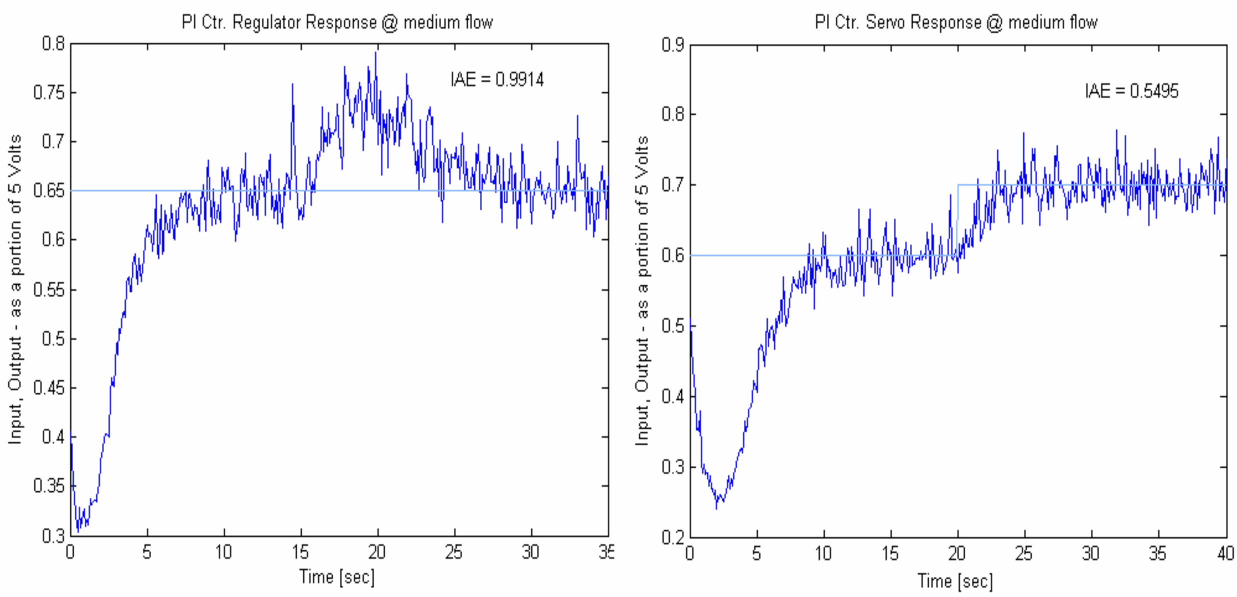

Figure 10: Responses – temperature system (with decoupling)

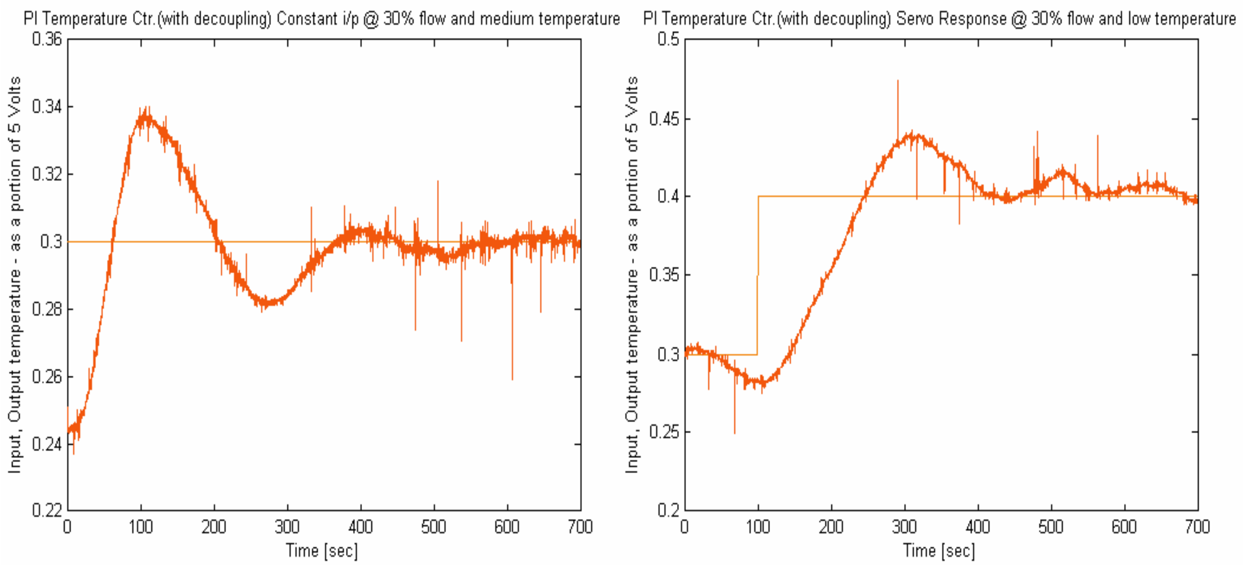

Figure 11: Regulator test – Flow system

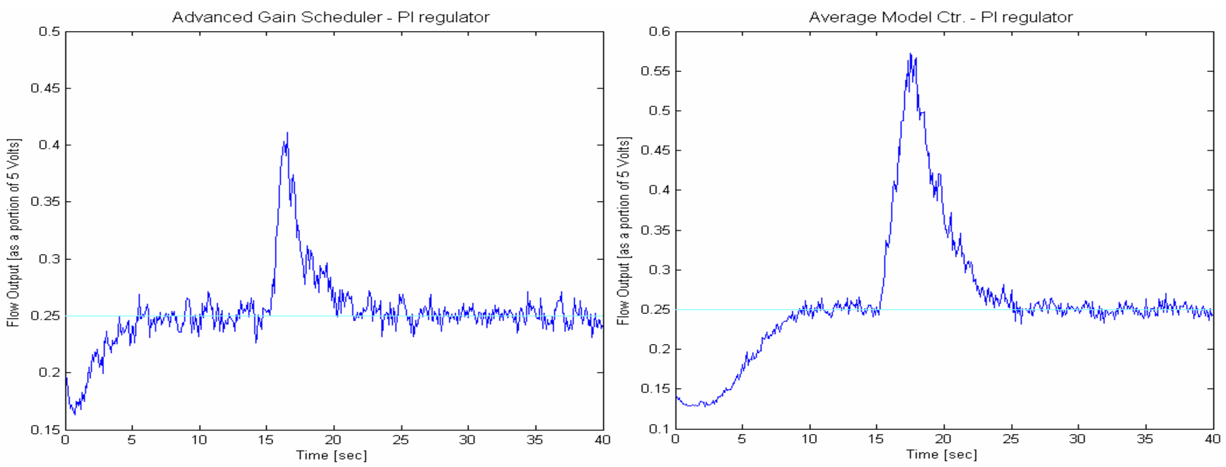

Figure 12: Servo test – Temperature system

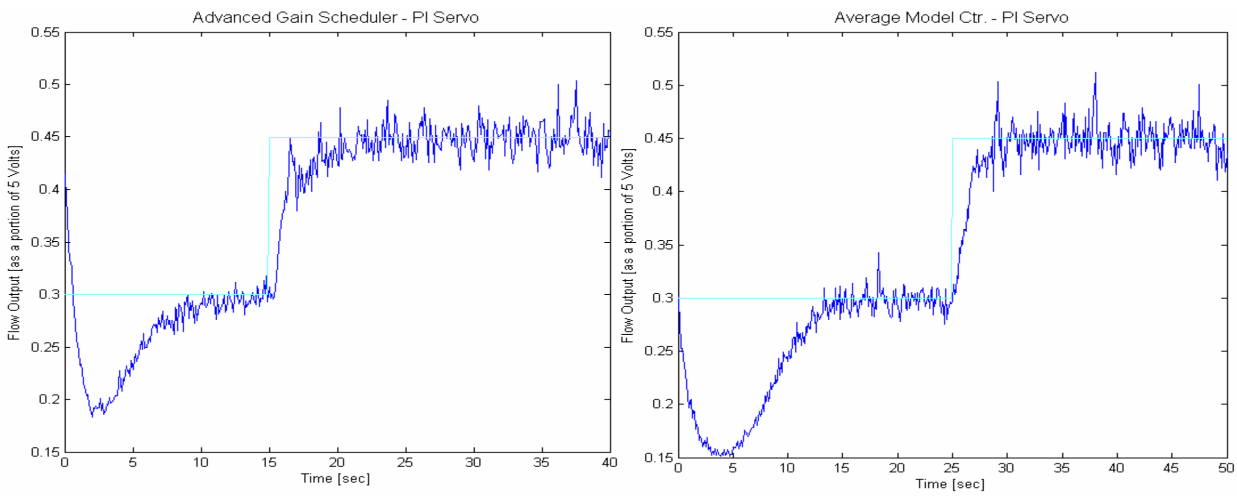

6. CONCLUSIONS AND RECOMMENDATIONS

The paper reports on the complete controller design cycle for a pilot scale heating and ventilation system. Starting by characterising the flow and temperature process at different operating points, simple FOLPD models are developed at each of these points. Interactive effects are explored and a decoupler is designed. PI and PID controllers are specified at each operating point, and gain scheduling is implemented to switch between the controllers. The implementation platform is based on HUMUSOFT/MATLAB/SIMULINK, with appropriate data acquisition. The results show satisfactory performance of the gain scheduler. The control solution could be improved by specifying a greater number of operating points for both the flow and temperature processes. The process modelling strategy, in addition, is not optimum as the responses exhibit considerable noise; the area-based step response modelling method, as described by Åström and Hägglund [10], would be a better choice.

REFERENCES

[1] Instrutek, Manual for VVS-400 – Heating and Ventilation Plant (1994).
[2] A.B. Rad, W.L. Lo and K.M. Tsang, Simultaneous online identification of rational dynamics and time delay: a correlation-based approach, *IEEE Trans. Control Syst. Tech.*, Vol. 11 (2003), 957-959.
[3] C.C. Chan, A.B. Rad and Y.K. Wong, Comparison of GPC controller and a PID auto-tuner for a heating plant, *Int. J. Elect. Enging. Educ.*, Vol. 34 (1997), 316-325.
[4] H.L. Ho, A.B. Rad, C.C. Chan and Y.K. Wong, Comparative study of three adaptive controllers, *ISA Trans.*, Vol. 38 (1999), 43-53.
[5] J.G. Ziegler and N.B. Nichols, Optimum settings for automatic controllers, *Trans. ASME*, (November 1942), 759-768.
[6] J.G. Ziegler and N.B. Nichols, Process lags in automatic control circuits, *Trans. ASME*, (July 1943), 433-444.
[7] D.E. Seborg, T.F. Edgar and D.A. Mellichamp, *Process Dynamics and Control*, Wiley, (1989).
[8] A. O'Dwyer, *Handbook of PI and PID Controller Tuning Rules*, Imperial College Press, London, U.K. (2003).
[9] R. Mooney, The estimation and control of a laboratory heating and ventilation process, *ME dissertation*, Dublin Institute of Technology (2003).
[10] K.J. Åström and T. Hägglund, *PID Controllers: Theory, Design and Tuning*, Second Edition, Instrument Society of America (1995).